

Evaluation of ANN and ANFIS Methods in Study of the Motion of a Bubble in A Combined Couette-Poiseuille Flow

Morteza Bayareh

Department of Mechanical Engineering,
Shahrekord University, Shahrekord, Iran
E-mail: m.bayareh@sku.ac.ir

Amireh Nourbakhsh*

Department of Mechanical Engineering,
Bu-Ali Sina University, Hamedan, Iran
E-mail: nourbakhsh@basu.ac.ir

*Corresponding author

Received: 11 March 2020, Revised: 18 June 2020, Accepted: 22 July 2020

Abstract: The equilibrium position of a deformable bubble in a combined Couette-Poiseuille flow is investigated numerically by solving the full Navier-Stokes equations using a finite-difference/front-tracking method. The present approach is examined to predict the migration of a bubble in a combined Couette-Poiseuille flow at finite Reynolds numbers of 5, 10, and 15. The related unsteady incompressible full Navier-Stokes equations are solved using a conventional finite-difference method with a structured staggered grid. The purpose of this study is to evaluate ANN and ANFIS methods in study of the lateral migration of the bubble. Evaluation criteria of accuracy in test set derived from ANFIS demonstrates that estimated values of correlation coefficient (r), Mean Absolute Error (MAE), and Root Mean Square Error (RMSE) are 0.97, 0.001, and 0.0014, respectively. The ANN model with RMSE of 0.0007, MAE of 0.0004 and r of 0.99, is better than ANFIS model. It is also demonstrated that the bubble position estimated by the ANN and ANFIS models closely follows the one achieved from front tracking method.

Keywords: ANN, ANFIS, Bubble, Front-Tracking Method, Reynolds Number

Reference: Morteza Bayareh, Amireh Nourbakhsh, "Evaluation of ANN and ANFIS Methods in Study of the Motion of a Bubble in A Combined Couette-Poiseuille Flow", Int J of Advanced Design and Manufacturing Technology, Vol. 14/No. 1, 2021, pp. 33–42. DOI: 10.30495/admt.2021.1895407.1180

Biographical notes: **Morteza Bayareh** received his PhD in Mechanical Engineering from Isfahan University of Technology. He is currently Associate Professor at the Department of Mechanical Engineering, Shahrekord University, Shahrekord, Iran. He was a postdoctoral researcher at University of Notre Dame, USA. His current research interest includes computational fluid dynamics, microfluidics and multiphase flows. He has published more than 50 journal papers and several conference ones. **Amireh Nourbakhsh** is Assistant Professor of Mechanical Engineering at Bu-Ali Sina University, Hamedan, Iran. She received her PhD in Mechanical engineering from Isfahan University of Technology. Her current research focuses on computational fluid dynamics and multiphase flows.

1 INTRODUCTION

The problem of particle motion in Couette and Poiseuille flows has been the subject of many numerical and experimental investigations. The flow of slurries, the recovery of oil by chemical flooding, food processing, and micro fluidic systems are typical application of these flows. Taylor [1] appears to be the first to have experimentally studied this phenomenon. The migration of neutrally buoyant solid particles was observed by Segre and Silberberg [2]. Their experimental results showed that the particles migrate away from both the wall and the centerline and accumulate at a certain equilibrium position of about 0.6 of the tube radius from the axis.

Karnis et al. [3] reported that neutrally buoyant particles stabilized midway between the centerline and the wall in a channel, closer to the wall for larger flow rates and closer to the center for larger particles. Halow and Wills [4] did experiments in a concentric cylindrical Couette device. They observed that when the inner cylinder rotates, a particle migrates from any initial position to equilibrium at a small distance inside the centerline of the gap. Zhou and Pozrikidis [5] studied the flow of periodic suspension of two dimensional viscous drops in a closed channel bounded by two parallel plane walls. Feng et al. [6] reported the results of a two-dimensional finite element simulation of the motion of a circular particle in Couette and Poiseuille flows. They showed that a neutrally buoyant particle migrates to the centerline in a Couette flow and exhibits the Segré-Silberberg effect in Poiseuille flow.

They discovered that several mechanisms are responsible for the lateral migration of rigid particles in shear flows: i) drift by the walls that mainly forces particles away from the walls, ii) migration of particles due to the effect of Inertia, provided that a slip velocity exists between the particle and the local undisturbed flow (the slip velocity is defined as the particle velocity minus the local undisturbed velocity at the center of the particle), and iii) migration due to the rotation of particle along with a slip velocity which is known as Magnus lift. In the Poiseuille flow, a lift force is caused by the velocity profile curvature. Saffman [7] found that, under creeping conditions, the inertial lift exerted on a spherical particle in an unbounded shear flow can be calculated as follows:

$$A = 6.4\rho Ua^2(\nu G)^{1/2} = 6.4\rho\nu Ua\text{Re}^{1/2} \quad (1)$$

Where, ν is the kinematic viscosity, U is the slip velocity of the particle and $\text{Re} = Ga^2/\nu$ is the Reynolds number defined based on the shear rate (G) and particle radius (a). Li et al. [8] studied the motion of two dimensional doubly periodic emulsions and foams by numerical simulations. Mortazavi and Tryggvason [9] studied the

motion of a single drop at finite Reynolds numbers in Poiseuille flow. They reported their results as a function of the Reynolds number, the Weber number and the viscosity ratio. They stated that at a small Reynolds number, the motion of the drop depends strongly on the viscosity ratio. Binary collision of drops and migration of a single drop in shear and Poiseuille flows have been described previously [10-18].

In recent years, new techniques such as Artificial Neural Network (ANN), Fuzzy Logic and Adaptive Neuro-Fuzzy Inference System (ANFIS) models have been applied for predicting in different fields and have attained better results than the traditional approaches (Nayak et al. [19], Chaves and Kojiri [20], and Zoveidavianpoor [21]).

In the present work, the flow is driven by a constant pressure gradient and constant velocity. Thus, the objective of this paper is to employ the finite difference/front tracking method to investigate the motion of a three-dimensional neutrally buoyant bubble between two parallel plates in a combined Couette-Poiseuille flow at finite Reynolds numbers. The main scope is to develop the ANN and ANFIS methods for accurately prediction of the effect of Reynolds number on the migration of a bubble in this flow. The results of the finite difference/front tracking method are compared with those of ANN and ANFIS methods.

2 GOVERNING EQUATIONS

The geometry of the flow is shown in “Fig. 1”. The motion of a bubble is studied in a channel that is bounded by two flat plates in the z -direction. The height and length of the channel are H . To decrease the computation time, the depth of the channel in the y -direction is taken to be $0.5H$. In absence of the bubble, the undisturbed flow is a combined Couette-Poiseuille flow. In Poiseuille flow, the flow is driven by a constant pressure gradient. For this problem [9]:

$$\nabla p = \nabla p_o + \nabla p' \quad (2)$$

Where, ∇p_o is the externally specified pressure gradient and $\nabla p'$ is the perturbation pressure gradient to be computed as part of the solution.

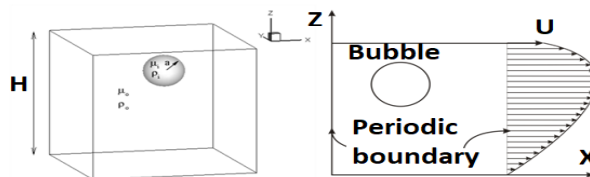


Fig. 1 The geometry for the simulation of a bubble in a combined Couette-Poiseuille flow.

The boundary condition on the plates is the no-slip boundary condition. The computational domain is periodic in the x- and y-directions. Normal stresses show the jump across the interface by surface tension and tangential stresses are continuous on the surface of the bubble

The governing non-dimensional numbers are as follows:

the ratio of the viscosity of the bubble fluid to the suspending medium $\lambda = \mu_i/\mu_o$, the density ratio $\alpha = \rho_i/\rho_o$, and the ratio of the radius of the bubble to the height of the channel $\zeta = a/H$. The viscosity and density of the bubble liquid are denoted by μ_i and ρ_i , respectively, and the suspending fluid has viscosity μ_o and density ρ_o . The bulk Reynolds number is defined in terms of the undisturbed channel centerline velocity U_c and the channel height, as $Re_b = \rho_o U_c H / \mu_o$. A Reynolds number based on the centerline velocity and the bubble diameter (d) is defined by $Re_d = \rho_o U_c d / \mu_o$. A particle Reynolds number can be defined as $Re_p = \rho_o U_c a^2 / \mu_o H$. The capillary number, $Ca = U_c \mu_o / \sigma$ describes the ratio of the viscous stress to the interfacial tension. Non-dimensional time is defined by $\tau = t U_c / H$.

One of the most important subjects considered by fluid mechanics researchers is flows with interfaces. Different numerical methods are used and developed for simulating these flows. These methods can be divided into two groups, depending on the type of grids used: moving grid and fixed grid. Two important approaches of fixed-grid methods, namely the Volume-of-Fluid (VOF) and level-set approaches, are among the most commonly used methods. The VOF method uses a marker function. The main difficulty in using VOF method has been the maintenance of a sharp boundary between the different fluids and the computation of the surface tension. The level-set method defines the interface by a level-set function, but this approach has some difficulties in preserving the mass conservation. Another method presented in this paper is the finite difference /front tracking method which improved the disadvantages of the previous methods. This approach was described in detail by Unverdi and Tryggvason [22-23] and only a brief outline is given here. The present computations are based on an improved implementation of the front tracking method at finite Reynolds numbers that include convective terms. The numerical technique is based on a direct discretization of the Navier-Stokes equation. In conservative form it is:

$$\frac{\partial \rho \mathbf{u}}{\partial t} + \nabla \cdot (\rho \mathbf{u} \mathbf{u}) = -\nabla p + \nabla \cdot \mu (\nabla \mathbf{u} + \nabla \mathbf{u}^T) - \int \sigma \kappa \mathbf{n} \delta(\mathbf{x} - \mathbf{x}') ds. \quad (3)$$

Where, \mathbf{u} is the velocity, p is the pressure, and ρ and μ are the discontinuous density and viscosity fields, respectively. σ is the surface tension coefficient, \mathbf{f} is a body force, and surface forces are added at the interface.

The term δ^β is a two- or three-dimensional δ function constructed by repeated multiplication of one-dimensional δ functions. The dimension is denoted by $\beta = 2$ or 3 , κ is the curvature for two-dimensional flow and twice the mean curvature for three-dimensional flows, \mathbf{n} is a unit vector normal to the front, \mathbf{x} is the point at which the equation is evaluated, and \mathbf{x}' is a Lagrangian representation of the interface.

This equation is solved by a second-order projection method using centred differences on a fixed regular, staggered grid. Both the bubble and the ambient fluid are taken to be incompressible, so the velocity field is divergence free [24]:

$$\nabla \cdot \mathbf{u} = 0. \quad (4)$$

Equation (4), when combined with the momentum equation, leads to a non-separable elliptic equation for the pressure. If the density is constant, the elliptic pressure equation is solved by fast Poisson solver (FISHPACK), but when the density of the bubble is different from the suspending fluid, the equation is solved by a multigrid method (Adams [25]).

Equations of state for the density and the viscosity are:

$$\frac{D\rho}{Dt} = 0, \quad \frac{D\mu}{Dt} = 0 \quad (5)$$

Where, D/Dt is the material derivative, and ‘‘Eq. (5)’’ simply states that the density and the viscosity of each fluid remain constant

3 RESULTS

In this section, the motion of a liquid bubble was studied at finite Reynolds numbers, and the effect of the Reynolds number are examined.

Figure 2a shows the non-dimensional lateral position of the bubble (z/H) versus the axial location for Reynolds numbers $Re_d = 5, 10, \text{ and } 15$ at $Ca = 0.3, \lambda = \alpha = 0.65$ and $\zeta = 0.125$. The grid resolution is $64 \times 32 \times 64$. The flow through the gap between the bubble and the wall leads to a repulsive lubrication force called ‘geometric blocking’ [6], that pushes the bubble away from the wall. The negative slip velocity and the curvature of the velocity profile generate a force that drives the bubble away from the center of the channel. Thus, these two forces move the bubble to an equilibrium position about halfway between the centerline and the wall according to the so-called Segre-Silberberg effect. As the Reynolds number increases, the inertia effect increases and effect of viscosity decreases. So, the lubrication force between the wall and bubble decreases and the equilibrium position moves slightly closer to the wall. The results are

in agreement with those reported by Schonberg and Hinch [26], Yang et al. [27], Asmolov [28], Mortazavi & Tryggvason [9] and Segre & Silberberg [2] for Poiseuille flow. The axial and slip velocities of the bubbles versus non-dimensional time are shown in “Fig. 2b & c”. As the Reynolds number increases, the axial velocities and slip velocities of the bubbles decrease. Figure 2d shows a slight increase of the bubble deformation with increasing Reynolds number, however, the bubble deformation is nearly the same at steady state equilibrium position.

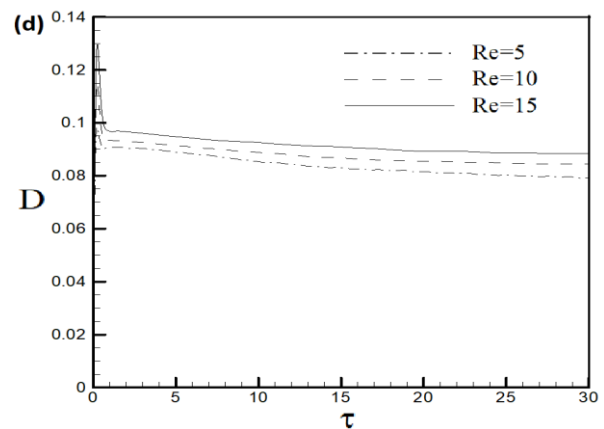
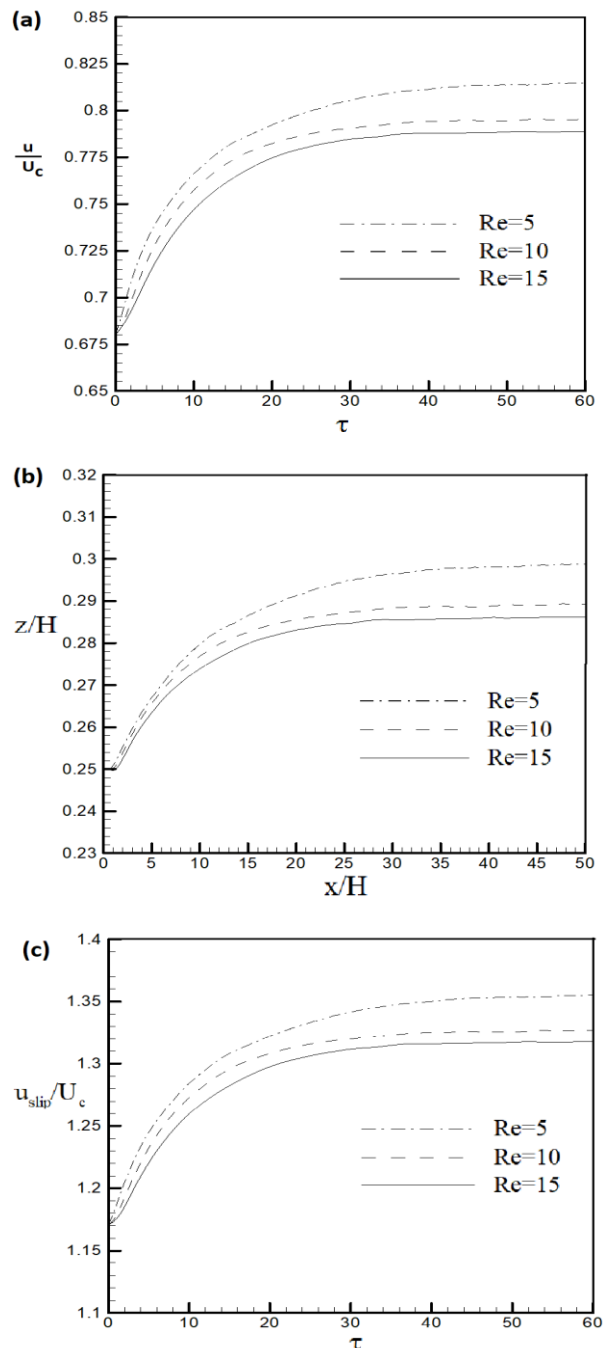


Fig. 2 (a): The lateral position versus the axial position, (b): axial velocity, (c): slip velocity and (d): bubble deformation versus non-dimensional time at three different Reynolds numbers.

4 ANN AND ANFIS METHODS

In this study, values of (Re), (X) and (T) were used as input variables and value of z/H that was estimated by front tracking method were used as output variable of ANN and ANFIS methods. Input and output variables of aforesaid were randomly divided into two parts of training and testing. In order to, a total of 75% of the available data set was reserved for training and the other 25% was used to testing the trained ANN and ANFIS. In addition, implementation of different structures for ANN and ANFIS methods were took by using MATLAB Software.

Artificial neural networks are new computational methods for learning based on data trends, gaining knowledge inherent in data, and knowledge extension for complex phenomenon. Artificial Neural Networks (ANNs) adaptability to hydrology is well described by ASCE [29] and Govindaraju and Rao [30]. With regard to capability of artificial neural networks in predicting nonlinear phenomena such as non-dimensional lateral position of the bubble (z/H), they are used here to predict non-dimensional lateral position of the bubble. Multilayer perceptrons (MLPs), as the best known type of neural networks, consist of input, hidden and output layers. The number of independent parameters affecting the outputs specifies the number of neurons in the input layer. The number of neurons in the hidden layer is determined by trial and error procedure or other techniques during the training process [31]. Linear, Sigmoid and Tanhporbolic (Tanh) activation functions and learning rules of Conjugate Gradient, Momentum and Levenberg Marquate are used in this study. Among the new techniques of modelling, fuzzy systems have a special place. The fuzzy expert system consists of linguistic rules relating the membership functions of the

input variables to the membership function of the output variable. A series of IF-THEN statements relates the input to the output variables. In this study, fuzzy logic was used as ANFIS method. The ANFIS model integrates adaptable fuzzy inputs with a modular neural network to rapidly and accurately approximate complex functions. Fuzzy inference systems are also valuable, as they combine the explanatory nature of rules (membership functions) with the power of ANNs. These types of networks solve problems more efficiently than ANNs when the underlying function to model is highly variable or locally extreme [32]. The characteristics of ANFIS are emphasized by the advantages of integrating ANNs with fuzzy inference systems (FIS) in the same topology [33]. The ANFIS architecture employed in this study is shown in “Fig. 3”.

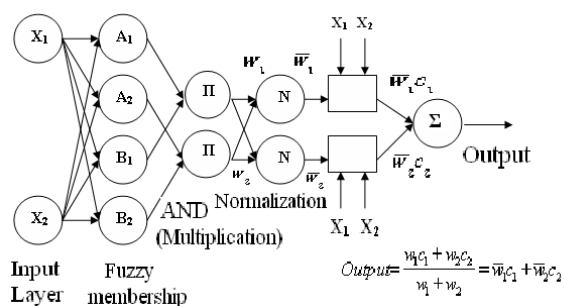


Fig. 3 A prototype two-input one-output ANFIS network and output calculation [24].

Takagi–Sugeno fuzzy structure [34] is preferred in this article. The Gaussian, Triangular, Trapezoidal and Generalized bell fuzzy types are used as membership functions to each input neuron. To evaluate the performance of the employed models in z/H estimates, several performance criteria were used including correlation coefficient (r), Root Mean Square Error (RMSE) and Mean Absolute Error (MAE). The r measures the degree to which two variables are linearly related and should optimally be one. The RMSE and MAE are criteria of the residual standard deviation and should be as small as possible (optimally zero). These criteria are defined in “Eqs. (10-12)”, respectively.

$$r = \frac{\left[\sum_{i=1}^n (X_i - \bar{X})(Y_i - \bar{Y}) \right]}{\sqrt{\sum_{i=1}^n (X_i - \bar{X})^2 \sum_{i=1}^n (Y_i - \bar{Y})^2}} \quad (6)$$

$$MAE = \frac{\sum_{i=1}^n |X_i - Y_i|}{n} \quad (7)$$

$$RMSE = \sqrt{\frac{\sum_{i=1}^n (X_i - Y_i)^2}{n}} \quad (8)$$

Where, X_i and Y_i are the i th observed and estimated values, respectively; \bar{X} and \bar{Y} are the average of X_i and Y_i , and n is the total numbers of data.

Sensitivity analysis is a testing process which provides a measure of the relative importance among the inputs of the neural model and illustrates how the model output varies in response to the variation of an input. The first input is varied from its mean by a predefined value of standard deviation while all other inputs are fixed at their respective means. The network output is computed for the predefined number of steps above and below the mean. This process is repeated until each input is considered once. A report is generated which summarizes the variation of each output with respect to the variation of each input [35-36].

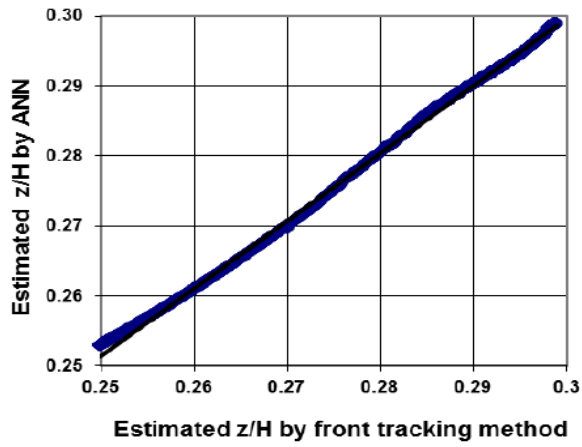
To use and test the ANN models, data is divided into a training set (in this study, 75% of the whole data) and a test set (25%). The training set is used to fit the ANN model weights (for a number of different network configurations and training phases) and the test set is used to evaluate the chosen model against unused data.

In this study, hundreds of different topologies are tested. This way of defining the topology takes a considerable amount of time, and it is nevertheless quite likely that an untested combination might have a better response to the expected generalization and convergence time than the one selected.

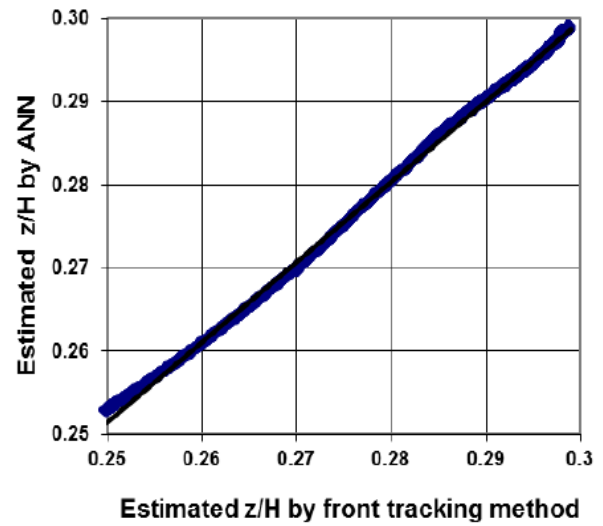
The statistical performance evaluation criteria of the ANN in training and testing phases are presented in Table 1. Although, several tests are repeated by using one, two and three hidden layers, a single hidden layer with seven neurons is the best architecture. The simulations show that increasing the number of hidden layers as well as the number of neurons in the hidden layers have no significant improvement in the estimated z/H. For the best selected architecture, the momentum learning algorithm and tanh activation function show the highest correlation coefficients and minimum errors. Different numbers of epochs are also tested to obtain the best case with minimum errors. For setting the numbers of epochs, the common practice is to start training with the default value of 1,000.

The results show that increase and decrease in this value brought nearly no significant improvement to the z/H estimate, and the default value is the optimum number for the best topology. Comparison of the z/H estimated by ANN and front tracking values at testing phases demonstrate good agreement (“Fig. 4”). As shown in “Table 1”, the best of ANN model has the smallest RMSE (0.0007), MAE (0.0004) and the highest r (0.99). In general, the present study confirms the capabilities of ANN as an effective tool for estimating z/H. These results are consistent with the results reported by Zoveidavianpoor [21]. Nourbakhsh et al. [29] also found that ANN is able to estimate a reasonable degree of accuracy.

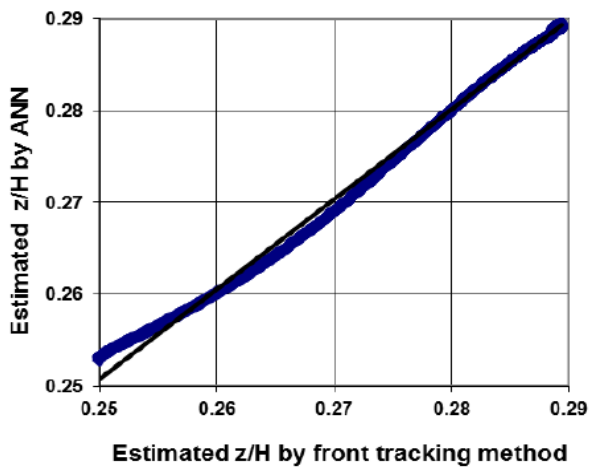
Training set (Re=5)



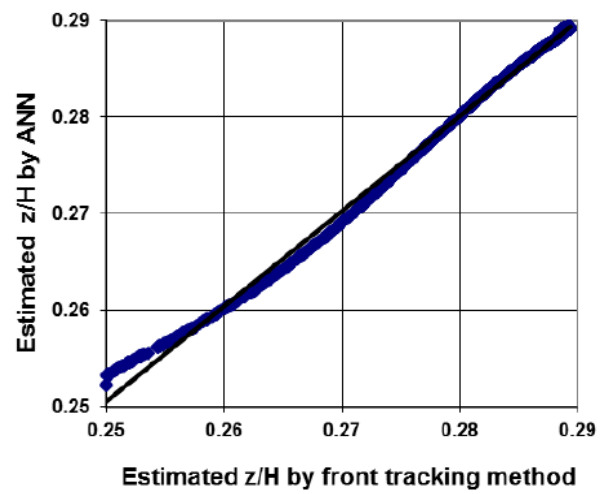
Test set (Re=5)



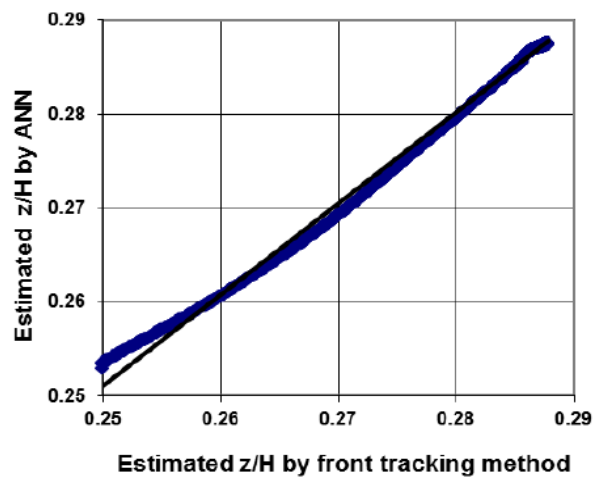
Training set (Re=10)



Test set (Re=10)



Training set (Re=15)



Test set (Re=15)

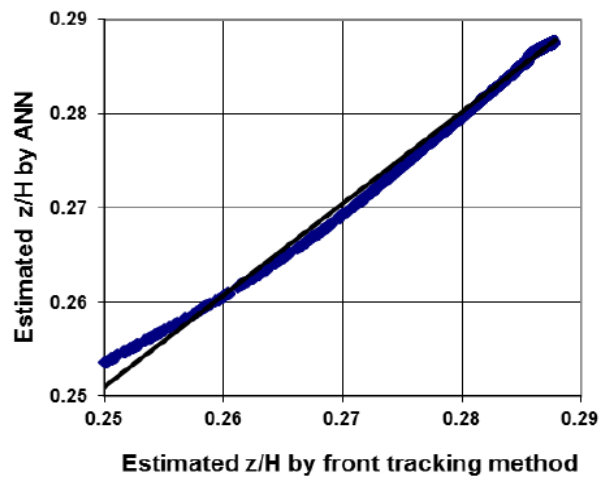


Fig. 4 Regression relationship between estimated z/H by ANN and front tracking.

Table 1 Statistical performance evaluation criteria of ANN in training and testing phases.

Activation function	Array	Training set			Test set		
		R	MAE	RMSE	R	MAE	RMSE
Tanh	3-6-1	0.99	0.0004	0.0007	0.99	0.0005	0.0010
Tanh	3-7-1	0.99	0.0003	0.0006	0.99	0.0004	0.0007
Sigmoid	3-5-1	0.98	0.0009	0.0019	0.97	0.0031	0.0068
Sigmoid	3-6-1	0.98	0.0009	0.0020	0.97	0.0031	0.0075
Linear	3-4-1	0.96	0.0016	0.0034	0.93	0.0094	0.0226
Linear	3-5-1	0.96	0.0017	0.0035	0.93	0.0106	0.0237
Tanh	3-2-3-1	0.98	0.0007	0.0008	0.97	0.0010	0.0011
Tanh	3-3-2-1	0.98	0.0007	0.0009	0.97	0.0009	0.0011
Sigmoid	3-2-3-1	0.98	0.0011	0.0029	0.97	0.0038	0.0078
Sigmoid	3-2-3-1	0.098	0.0012	0.0029	0.97	0.0038	0.0078
Linear	3-2-2-1	0.95	0.0021	0.0051	0.9	0.0300	0.0260
Linear	3-2-2-1	0.95	0.0022	0.0055	0.9	0.0301	0.0280

The ANFIS’s architecture comprises of three (3) inputs and one output. Different ANFIS architectures are tried using this code and the appropriate model structures are determined for each input combination. Then, the ANFIS models are tested and the results are compared by means of performance statistics. The results of

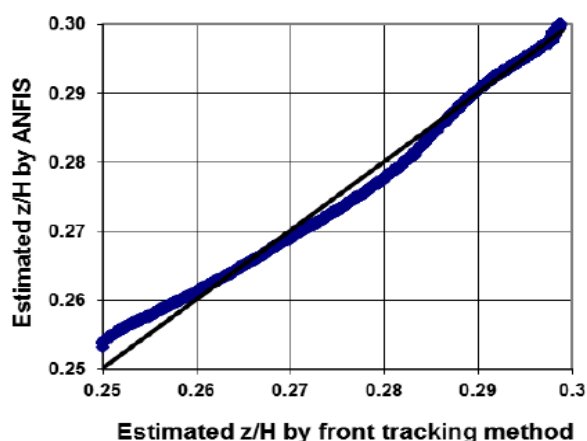
statistical evaluation criteria of the ANFIS model for estimation of z/H are presented in “Table 2”. The final ANFIS architecture is attained by Triangular membership function with 2-3-3 arrays (for input variable of Re, X and T, respectively).

Table 2 Statistical performance evaluation criteria of ANFIS in training and testing phases.

Membership function	Array	Training set			Test set		
		R	MAE	RMSE	R	MAE	RMSE
Triangular	2-3-3	0.98	0.0008	0.0012	0.97	0.0010	0.0014
Trapezoidal	4-3-3	0.98	0.0011	0.0017	0.97	0.0013	0.0022
Generalized bell	2-3-3	0.98	0.0013	0.0027	0.96	0.0015	0.0039
Gaussian	3-3-3	0.98	0.0014	0.0047	0.97	0.0019	0.0051

The comparison of the front tracking values and estimated z/H , by the best of ANFIS model is shown in “Fig. 5”.

Training set (Re=5)



Training set (Re=10)



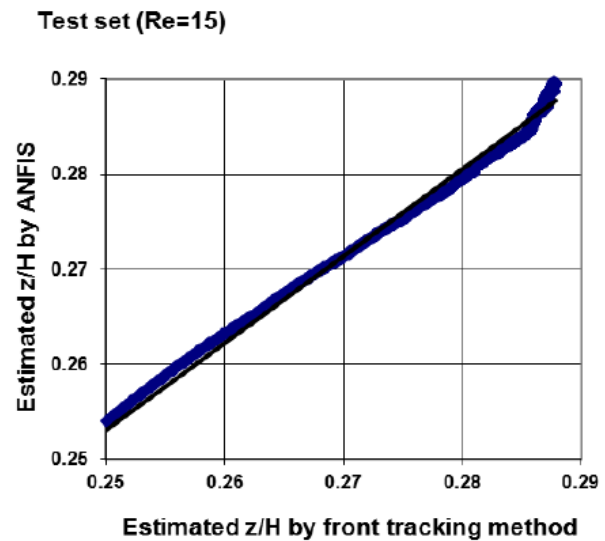
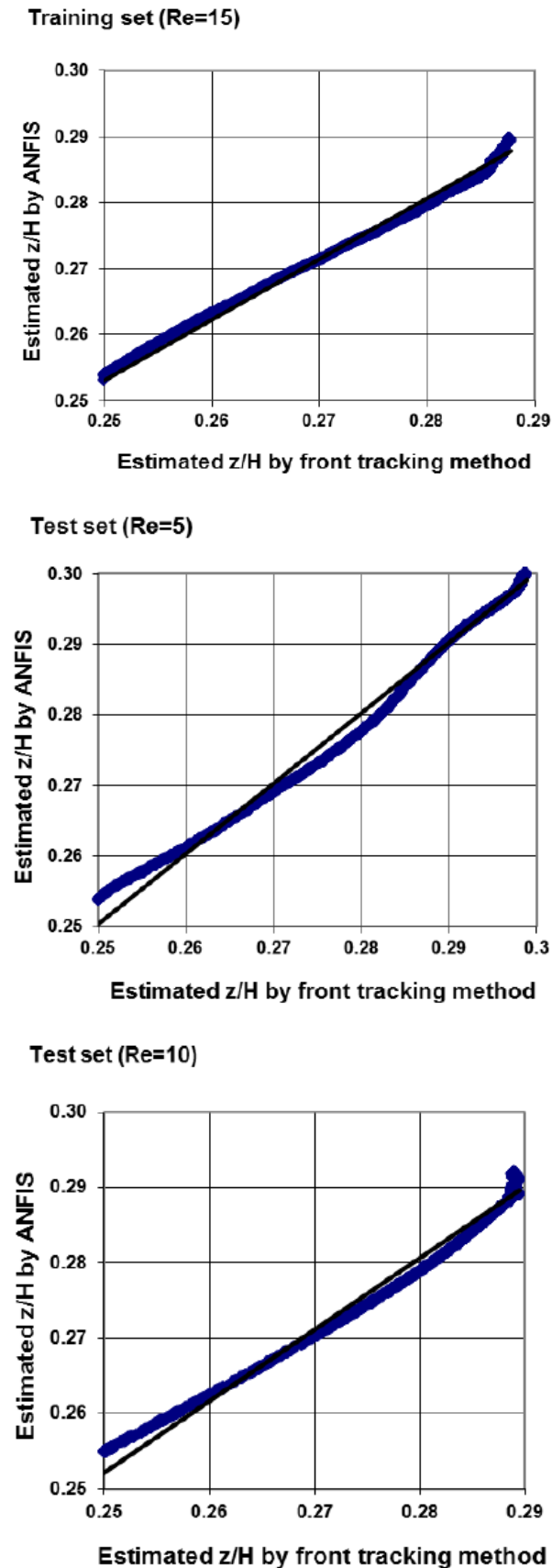


Fig. 5 Regression relationship between estimated z/H by ANFIS and front tracking.

It is seen from the scatterplots that the z/H values estimated by the ANFIS models closely follow the front tracking values and ANFIS can be successfully applied to establish the estimating models that could provide accurate and reliable z/H estimation. Evaluation criteria of accuracy in test set derived from ANFIS demonstrates that estimated values of r, MAE and RMSE are 0.97, 0.0010 and 0.0014, respectively (“Table 2”). Also, the final architectures of the ANN model show itself upper accuracy related to ANFIS model for estimation of z/H. The obtained results are supported by the other study [21], [37-38].

The results of sensitivity analysis of the z/H variables are given in “Table 3”. In this table, variation of z/H (%) with respect to the variation in each input is presented. It is obvious that increase in Re, X and T is significant at 35.21, 10.08 and 6.16 levels, respectively. Re and X are the most sensitive variables. In other words, variation of Re and X causes the most percent change of z/H.

Table 3 The sensitivity of z/H to the input variables.

Sensitivity	z/H (%)
Re	35.21
X	10.08
T	6.11

5 CONCLUSION

In the present study, a finite difference/ front tracking method is used for simulation of the motion of a three-dimensional neutrally buoyant bubble between two parallel plates in a combined Couette-Poiseuille flow at finite Reynolds numbers. The bubble migrates to an equilibrium lateral position about halfway between the

centerline and the wall according to the so-called Segre-Silberberg effect. As the Reynolds number increases, the equilibrium position moves slightly closer to the wall.

The objective of this paper is to develop the ANN and ANFIS methods for accurately predicting the effect of Reynolds number on the migration of a bubble in a combined Couette-Poiseuille flow and comparing the results of the finite difference/front tracking method and the ANN and ANFIS methods. The potential of ANN and ANFIS in estimation of the lateral position (z/H) is investigated.

The results reveal that ANN and ANFIS could satisfactorily bring into play for estimation of z/H . The ANN model with RMSE of 0.0007, MAE of 0.0004 and r of 0.99, is better than ANFIS model. It is concluded that the z/H values estimated by the ANN and ANFIS models closely follow the front tracking values. The results of sensitivity analysis to variables show that Re and X are the most sensitive variables. It should be noted that the results obtained in this study are valid for the presented data set and one might not obtain the same behavior for other ones. For further work, using more data may be required to provide additional support for these conclusions. Finally, as a recommendation for future study, additional studies should be conducted to recognize and evaluate the effects of the other conventional well log parameters on z/H .

REFERENCES

- [1] Taylor, G. I., The Deformation of Emulsions in Definable Fields of Flow, *Proceeding of The Royal Society*, Vol. A146, 1934, pp. 501–523.
- [2] Segre, G., Silberberg, A., Behavior of Macroscopic Rigid Spheres in Poiseuille Flow Part 2. Experimental Results and Interpretation, *Vol. 14, No. 1, 1962*, pp. 136-157.
- [3] Karnis, A., Mason, S. G., Particle Motions in Shear Suspension, Part 3. Wall Migration of Fluid Drops, *Colloid Interface Science*, Vol. 24, 1967, pp. 164-169.
- [4] Halow, J. S., Willis, G. B., Radial Migration of Spherical Particles in Couette System, *AICHE Journal*, Vol. 16, 1970, pp. 281-286.
- [5] Zhou, H., Pozrikidis, C., The Flow of Suspensions in Channels: Single Files of Drops, *Physics of Fluids*, Vol. 2, 1993, pp. 311-324.
- [6] Feng, J., Hu, H. H., and Joseph, D. D., Direct Simulation of Initial Value Problems for the Motion of Solid Bodies in a Newtonian Fluid, Part2. Couette Flow and Poiseuille Flows, *Journal of Fluid Mechanics*, Vol. 277, 1994, pp. 271–301.
- [7] Saffman, P. G., The Lift On a Small Sphere in A Slow Shear Flow, *Journal of Fluid Mechanics*, Vol. 22, 1965, pp. 385-400.
- [8] Li, X., Zhou, H., and Pozrikidis, C., A Numerical Study of the Shearing Motion of Emulsions and Foams, *Journal of Fluid Mechanics*, Vol. 286, 1995, pp. 374–404.
- [9] Mortazavi, S., Tryggvason, G., A Numerical Study of the Motion of Drop in Poiseuille Flow Part1: Lateral Migration of One Drop, *Journal of Fluid Mechanics*, Vol. 411, 2000, pp. 325–350.
- [10] Goodarzi, Z., Ahmadi Nadooshan, A., and Bayareh, M., Numerical Investigation of Off-Center Binary Collision of Droplets in A Horizontal Channel, *Journal of the Brazilian Society of Mechanical Sciences and Engineering*, Vol. 40, 2018, pp. 1-10. <http://dx.doi.org/10.1007/s40430-018-1075-y>
- [11] Armandoost, P., Bayareh, M., and Ahmadi Nadooshan, A., Study of the Motion of a Spheroidal Drop in A Linear Shear Flow, *Journal of Mechanical Science and Technology*, Vol. 32, 2018, pp. 2059-2067. <http://dx.doi.org/10.1007/s12206-018-0415-2>
- [12] Bayareh, M., Mortazavi, S., Effect of Density Ratio On the Hydrodynamic Interaction Between Two Drops in Simple Shear Flow, *Iranian Journal of Science and Technology*, Vol. 35, 2011, pp. 441-452. DOI: 10.22099/ijstm.2011.900
- [13] Bayareh, M., Mortazavi, S., Equilibrium Position of a Buoyant Drop in Couette and Poiseuille Flows at Finite Reynolds Numbers, *Journal of Mechanics*, Vol. 29, 2013, pp. 53-58. <http://dx.doi.org/10.1017/jmech.2012.109>
- [14] Bayareh, M., Mortazavi, S., Geometry Effects On the Interaction of Two Equal-Sized Drops in Simple Shear Flow at Finite Reynolds Numbers, 5th International Conference: Computational Methods in Multiphase Flow, *WIT Trans. Eng. Sci.*, Vol. 63, 2009, pp. 379-388.
- [15] Bayareh, M., Mortazavi, S., Migration of a Drop in Simple Shear Flow at Finite Reynolds Numbers: Size and Viscosity Ratio Effects, *Proceeding of International Conference on Mechanical, Industrial and Manufacturing Engineering (ICMIME)*, Cape Town, South Africa, 2010.
- [16] Mohammadi Masiri, S., Bayareh, M., and Ahmadi Nadooshan, A., Pairwise Intercation of Drops in Shear-Thinning Inelastic Fluids, *Korea-Australia Rheology Journal*, Vol. 31, No. 1, 2019, pp. 25-34. <https://doi.org/10.1007/s13367-019-0003-8>
- [17] Bayareh, M., Nourbakhsh, A., Study of the Bubble Motion in A Compound Couette-Poiseuille Flow: Effect of The Pressure Gradient, *Advances in Modelling and Analysis A*, Vol. 55, No. 1, 2018, pp. 11-19. https://doi.org/10.18280/ama_a.550102
- [18] Bayareh, M., Dabiri, S., and Ardekani, A. M., Interaction Between Two Drops Ascending in A Linearly Stratified Fluid, *European Journal of Mechanics-B/Fluids*, Vol. 60, 2016, pp. 127-136. <http://dx.doi.org/10.1016/j.euromechflu.2016.07.002>
- [19] Nayak, P. C., Sudheer, K. P., Rangan, D. M., and Ramasastry, K. S., A Neuro-Fuzzy Computing Technique for Modeling Hydrological Time Series, *Journal of Hydrology*, Vol. 291, 2004, pp. 52-66.

- [20] Chaves, P., Kojiri, T., Deriving Reservoir Operational Strategies Considering Water Quantity and Quality Objectives by Stochastic Fuzzy Neural Networks, *Advances in Water Resources*, Vol. 30, 2007, pp. 1329-1341.
- [21] Zoveidavianpoor, M., A Comparative Study of Artificial Neural Network and Adaptive Neurofuzzy Inference System for Prediction of Compressional Wave Velocity, *Neural Computing and Applications*, Vol. 25, 2014, pp. 1169-1176
- [22] Unverdi, S. O., Tryggvason, G., A Front-Tracking Method for Viscous Incompressible Multi-Fluid Flows, *Journal of Computational Physics*, Vol. 100, 1992, pp. 25-82
- [23] Unverdi, S. O., Tryggvason, G., Computations of Multi-Fluid Flows, *Physics*, Vol. D60, 1992, pp. 70-83
- [24] Tryggvason, G., Bunner, B., Esmaeeli, A., Juric, D., Al-Rawahi, N., Tauber, W., Han, J., Nas, S., and Jan, Y. J., A Front-Tracking Method for the Computations of Multiphase Flow, *Journal of Computational Physics*, Vol. 169, 2001, pp. 708-759
- [25] Adams, J., MUDPACK: Multigrid FORTRAN Software for The Efficient Solution of Linear Elliptic Partial Differential Equations, *Applied, Mathematics and Computation*, Vol. 34, 1989, pp. 113-146
- [26] Schonberg, J. A., Hinch, E. J., Inertial Migration of a Sphere in Poiseuille Flow, *Journal of Fluid Mechanics*, Vol. 203, 1989, pp. 517-524
- [27] Yang, B. H., Wang, J., Joseph, D. D., Hu, H. H., Pan, T. W., and Glowinski, R., Migration of a Sphere in Tube Flow, *Journal of Fluid Mechanics*, Vol. 540, 2005, pp. 109-131
- [28] Asmolov, E. S., The Inertial Lift On a Spherical Particle in A Plane Poiseuille Flow at Large Channel Reynolds Number, *Journal of Fluid Mechanics*, Vol. 381, 1999, pp. 63-87
- [29] ASCE Task Committee on Application of Artificial Neural Networks in Hydrology. Artificial neural networks in hydrology: I. Preliminary Concepts, *Journal of Hydraulic Engineering*, Vol. 5, No. 2, 2000, pp. 124-137.
- [30] Govindaraju, R. S., Rao, A. R., *Artificial Neural Networks in Hydrology*, Kluwer Academic Publishers, Amsterdam, the Netherlands, 2000.
- [31] Nasseh, S., Mohebbi, A., Sarrafi, A., and Taheri, M., Estimation of Pressure Drop in Venturi Scrubbers Based On Annular Two-Phase Flow Model, *Artificial Neural Networks and Genetic Algorithm*, *Chemical Engineering Journal*, Vol. 150, 2009, pp. 131-138
- [32] Parthiban, L., Subramanian, R., Intelligent Heart Disease Prediction System using CANFIS and Genetic Algorithm, *International Journal of Biological and Medical Sciences*, Vol. 3, 2008, pp. 157-160
- [33] Aytek, A., Co-Active Neurofuzzy Inference System for Evapotranspiration Modeling, *Soft Computing-A Fusion of Foundations, Methodologies and Applications*, Vol. 13, No. 7, 2008, pp. 691-700
- [34] Takagi, T., Sugeno, M., Fuzzy Identification of Systems and Its Applications to Modeling and Control, *IEEE Transactions on Systems*, Vol. 15, No. 1, 1985, pp. 116-132
- [35] Jalali-Heravi, M., Asadollahi-Baboli, and M., Shahbazikhah, P., QSAR Study of Heparanase Inhibitors Activity Using Artificial Networks and Levenberg-Marquardt Algorithm, *European Journal of Medicinal Chemistry*, Vol. 43, 2008, pp. 548-556
- [36] Tabari, H., Marofi, S., and Sabziparvar, A. A., Estimation of Daily Pan Evaporation Using Artificial Neural Network and Multivariate Non-Linear Regression, *Irrigation Science*, Vol. 28, 2010, pp. 399-406
- [37] Nourbakhsh, A., Ghahremani, Z., and Zojaji, M., Entropy Generation Minimization of a MHD Flow over a Rotating Disk using Artificial Neural Network and Artificial Bee Colony, *Majlesi Journal of Energy Management*, Vol. 3, No. 4, 2014, pp. 29-40
- [38] Piri, J., Mohammadi, K., Shamshirband, S., and Akib, S., Assessing the Suitability of Hybridizing the Cuckoo Optimization Algorithm with ANN and ANFIS Techniques to Predict Daily Evaporation, *Environmental Earth Sciences*, Vol. 75, No. 3, 2016, pp. 1-13.